MANUFACTURING PROCESS AND MECHANICAL PROPERTIES OF CARBON FIBER/CARBON NANOTUBE BUCKYPAPER INTERPLY HYBRID COMPOSITES

Ayou Hao*, Songlin Zhang, Nam Nguyen, Liyu Dong, Claire Jolowsky, Rebekah Downes Sweat, Jin Gyu Park and Zhiyong Liang

High-Performance Materials Institute, Florida State University, 2005 Levy Ave, Tallahassee, FL 32310, USA, E-mail: ahao@fsu.edu

Keywords: Polymer-matrix composites (PMCs); Carbon fiber/carbon nanotube hybrid; Autoclave; Mechanical properties

ABSTRACT

This paper reports on a study of CNT thin film or buckypaper (BP), integrated into carbon fiber (CF) prepreg composites to create hybrid composite materials with high CNT content. Three different CNT materials are used: (1) commercial available buckypaper supplied by Nanocomp Inc. USA, (2) continuous buckypaper made in-house by sonication suspension method and (3) in-house growth CNT using floating catalyst chemical vapor deposition (FCCVD) method. The advantages of this research lie in four aspects: (1) high global CNT loading (up to 5 wt%), (2) increased sample size (203×178 mm^2) and efficient fabrication method, (3) the use of aerospace-grade high-performance resin system (CYCOM 5250-4 bismaleimide resin supplied by Cytec Engineering Materials) and (4) comprehensive characterizations including axial tensile and flexural tests, as well as three-axis electrical conductivities. They are the keys to further studying and demonstrating the engineering performance of CNT/CF hybrid composites for high-performance aerospace structural applications. The autoclave process of manufacturing hybrid composite laminates was investigated to gain an understanding of nano/micro dual-scale resin flow characteristics. The study found that resin bleeding along the through-thickness direction was inhibited due to extra-low permeability and high resin absorbing capacity of the buckypaper. Resin matrix-impregnated buckypaper layers were much thicker than dry pristine buckypaper due to high resin absorbency and swelling effects. Surface functionalization has been applied on the BP to improve the CNT/CF and CNT/resin interfacial bonding. The CVD-buckypaper/unidirectional carbon fiber (UD-CF) hybrid composites had average tensile strength of 2978 MPa and average flexural strength of 2183 MPa. The dramatic improvements in axial, transverse and through-thickness electrical conductivities demonstrate potential for multifunctional applications such electro-magnetic interface (EMI) shielding of the resultant hybrid composites.

1 INTRODUCTION

Lightweight and corrosion-resistant nonmetal electrical conductors are highly desired for applications in aerospace, portable electronics, medical devices and marine instruments [1]. Due to the extraordinary attributes of carbon nanotubes (CNTs), including low density, one dimensional structure, tunable electrical properties and mechanical strength/stiffness exceeding any other conductive metals, CNTs have been extensively studied at different scales from nanoscale individual CNTs to macroscale CNT assemblies, such as yarns (also referred to as fibers), sheets (such as buckypaper) or ribbons for electrical conduction applications [2–5]. Although the electrical conductivity of an individual CNT could be as high as 10^6 S/cm for single-walled CNTs (SWNTs) and 3.3×10^4 S/cm for multi-walled CNTs (MWNTs) [6], macroscopic CNT assemblies showed limited conductivity due to the discontinuity, misalignment, loose packing, and impurities, which profoundly impacts the electrons or charge carriers transport due to scattering effect and contact resistance between individual tubes and bundles [4]. A crystal packing

structure of CNT assemblies with good alignment leads to a small contact resistance and facilitates the charge carriers transferring among individual nanotubes, and bundles of CNT networks of sizable CNT sheets and tapes [7]. Carbon fiber (CF) polymer matrix composites (PMCs) have been increasingly used as advanced structural materials in aerospace, military and industrial applications [5,8–10]. CNTs have been applied in composite materials as fillers in resin matrices [1] or by direct growth on fiber surfaces to improve structural, electrical, and thermal properties [2] due to their attractive properties. However, homogeneous dispersion of CNTs and fabrication of excellent-quality composites with high CNT contents in large-scale structures remain major technological challenges [3,11]. Buckypaper presents an effective way of introducing CNTs into composites, as it is a freestanding mat of densely-packed and inter-tangled CNTs [4]. Due to its high CNT concentration, buckypaper provides great advantages to enhance electrical properties [5], actuation [6], flame retardancy [7,12] and electromagnetic interference (EMI) shielding properties [13]. Buckypaper can be produced in large sizes and provides ease of handling and improves the safety of using CNTs in industrial manufacturing facilities [14]. These features make buckypaper an excellent candidate for manufacturing large scale composite samples with CF prepreg to achieve high CNT loading.

2 MATERIALS AND EXPERIMENTS

2.1 MATERIALS AND CONDUCTIVE CNT SHEETS PREPARATION

Commercially available carbon nanotube sheets (NC-BP) were purchased from Nanocomp Technologies Inc. (NH, USA). Continuous buckypaper (FSU-BP) was made in-house by sonication suspension method and in-house growth CNT BP (CVD-BP) was using floating catalyst chemical vapor deposition (FCCVD) method. Cytec Engineered Materials Inc. supplied the unidirectional IM7/CYCOM® 5250-4 prepreg, which had an areal density of 210 g/m^2 and a resin content of ~32wt%.

2.2 FABRICATION OF BP/CF INTERPLY HYBRID COMPOSITES

Figure 1 shows the manufacturing process of the hybrid composites. In the lay-up process, carbon fiber prepreg and buckypaper materials were laminated according to a designed stacking sequence on a steel mold. The overall lay-up sequence from the bottom-to-top on the mold-surface was in the following order: release film, interply hybrid structure made of alternating carbon fiber and buckypaper layers, peel ply, caul plate, breather and vacuum bagging film, as shown in Figure 1 (c). The assembly was finally vacuum- bagged under a full vacuum to expel air. BP/CF hybrid composites were cured using an autoclave process, shown in Figure 1 (e) following the CYCOM 5250-4 curing schedule, followed by a post-cure process at 227 °C for 4 hours. Figure 1(d) shows the in-house made large size BP/CYCOM 5250-4 prepreg. Table 1 shows the sample layup design. Carbon fiber prepreg was 203×178 mm^2 and BP prepreg was 152×152 mm^2.

2.3 CHARACTERIZATION

Tensile tests were conducted following the ASTM D 3039 standard using an MTS Landmark test system. A non-contact video extensometer monitored and recorded the specimen strain to calculate the tensile modulus. The specimens were 13×203 mm^2. E-glass fiber reinforced epoxy tabs were used for the testing samples. The crosshead speed of the test machine was 1mm/min. Flexural tests were conducted following ASTM D790 in three-point bending mode on a SHIMADZU AGS-J tester with crosshead speed of 1 mm/min. Sample size was 13×51 mm^2 Electrical property measurements were conducted using a current source (Keithley 6221) and nanovoltmeter (Keithley 2182A) in a four-probe configuration. The sample surface was coated with a gold layer and observed using a SEM machine (JEOL JSM-7401F USA, Inc.).

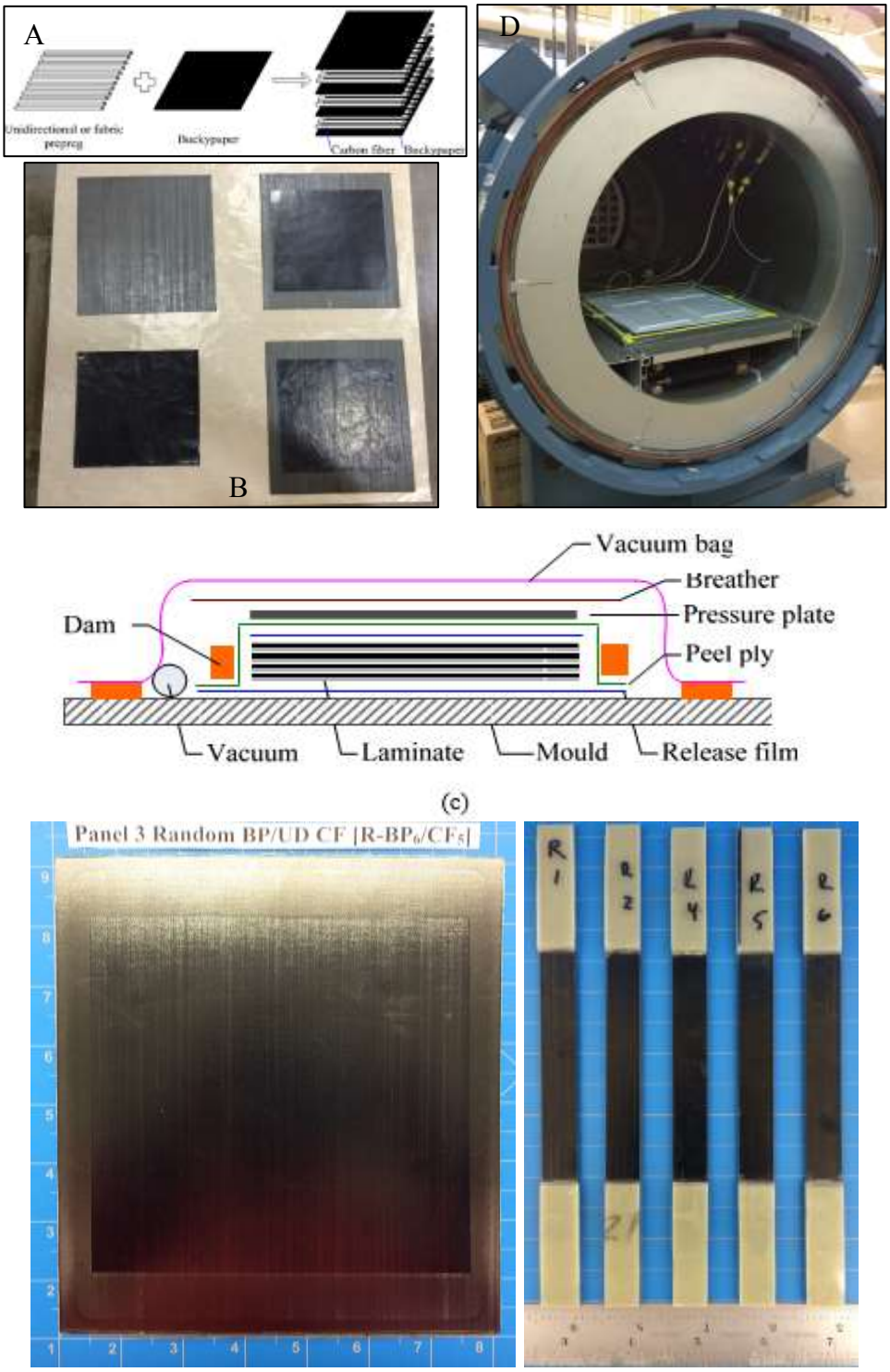

Figure 1. (a) Stacking schematic of hybridization of buckypaper and carbon fiber, (b) hybrid prepregs, (c) vacuum bag setup, (d) the autoclave curing setup and (e) finished composite panel and tensile test coupons

Table 1. Structural parameters of BP/CF interply hybrid composites

Composite panel #	Name	Lay-up
1	UD CF control	$[UD\text{-}CF]_6$
2	NC-BP control	$[NC\text{-}BP]_6$
3	NC-BP/CF hybrid	$[(BP/CF)_2/\ BP/\overline{CF}]_s$
4	Functionalized NC-BP/CF hybrid	
5	FSU-BP/CF hybrid	
6	CVD-BP/CF hybrid	

2. RESULTS AND DISCUSSION

2.1. HYBRID COMPOSITE QULITY

To study the consistent quality of the hybrid and corresponding control panels, C-scan imaging was performed to detect any voids or resin rich areas. Figure 2 shows each panel, where resin rich areas are denoted by lighter green areas and void areas are shown by notably dark areas in the images. The C-scan images in Figure2 begin by denoting a consistent and classic aerospace-grade quality of good adhesion between laminas in the case of the (a) CF-control, (c) the NC-BP/CF hybrid and the (d) functionalized NC-BP/CF hybrid with only minor flaws due to buckypaper flow barrier properties. There is noted horizontal resin flow orientation due to the UD-CF used, but resin consistency is found. The BP control in Figure 2 (b) shows patterned resin rich areas due to the random nature of the CNTs that do not have CF as a supporting structure for resin flow.

The composite quality was evaluated by SEM analysis. Figure 3 shows typical cross-sections observed in the hybrid composites and control samples. Cartoon illustrations are also added to the left of the SEM cross-section to illustrate varied layer thicknesses for the three different BP cases. The SEM images in Figure 4 clearly show that the composition of the constituent parts of the hybrids, including CF, BMI resin and BP, vary among the NC-BP, FSU-BP and CVD-BP cases. Defects were found to closely correlate to the buckypaper incorporation and the resultant thickness increases that buckypaper samples possess.

Resin-starved regions and voids were found to be the most common defects in the BP/CF hybrid composites. The resin-starvation defects were directly related to the high resin absorbency of the buckypaper layers and thick buckypaper-based hybrid laminates. A closer look at the hybrid cross-sections in Figure 4 reveal consistent thickness and low void content, especially for the NC-BP case. From the resultant cross-sectional morphology, shown in Figure 4 (g,h), when CVD-BP layers are introduced, resin-starvation defects tended to appear within the carbon fiber laminas. This type of defect is due to stronger capillary forces in the buckypaper layers compared to that of the carbon fiber networks – a result of the even smaller nanoscale capillary radius of aligned BP as compared to random BP [15]. The resin was absorbed into the buckypaper layer, leading to CF layer resin- starvation. When resin-starvation defects occurred, little resin bleeding was observed at the laminate edges in the alignment direction during the fabrication process.

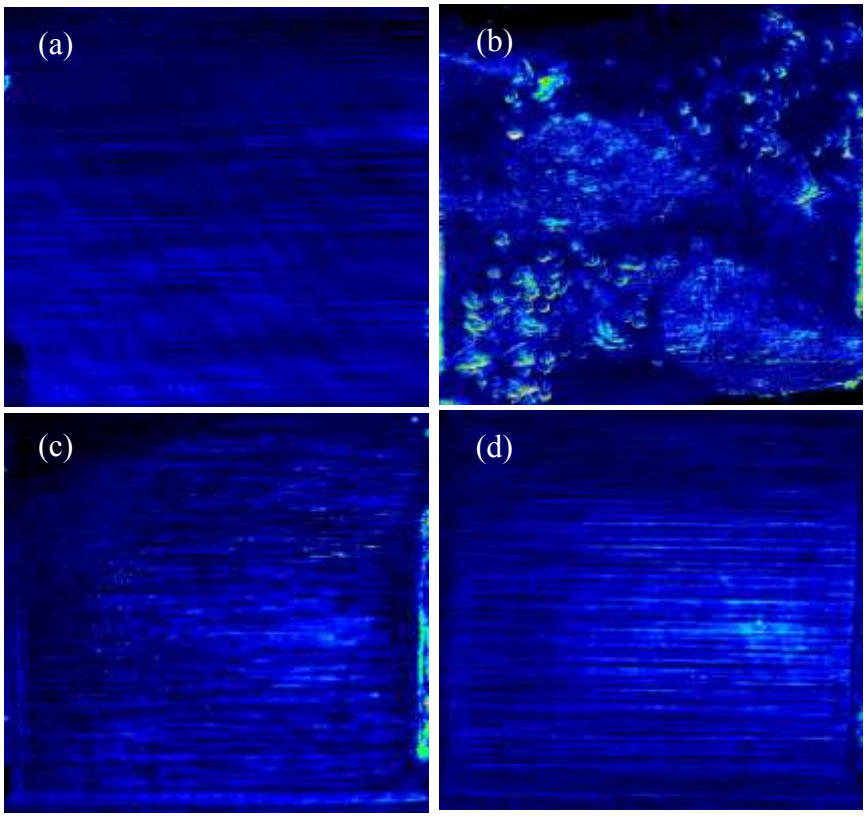

Figure 2. C-scan images of (a) Panel #1: the CF control, (b) Panel #2: BP control, (c) Panel #3: NC-BP hybrid and (d) Panel #4: functionalized NC-BP hybrid composites, which show resin flow and defect areas

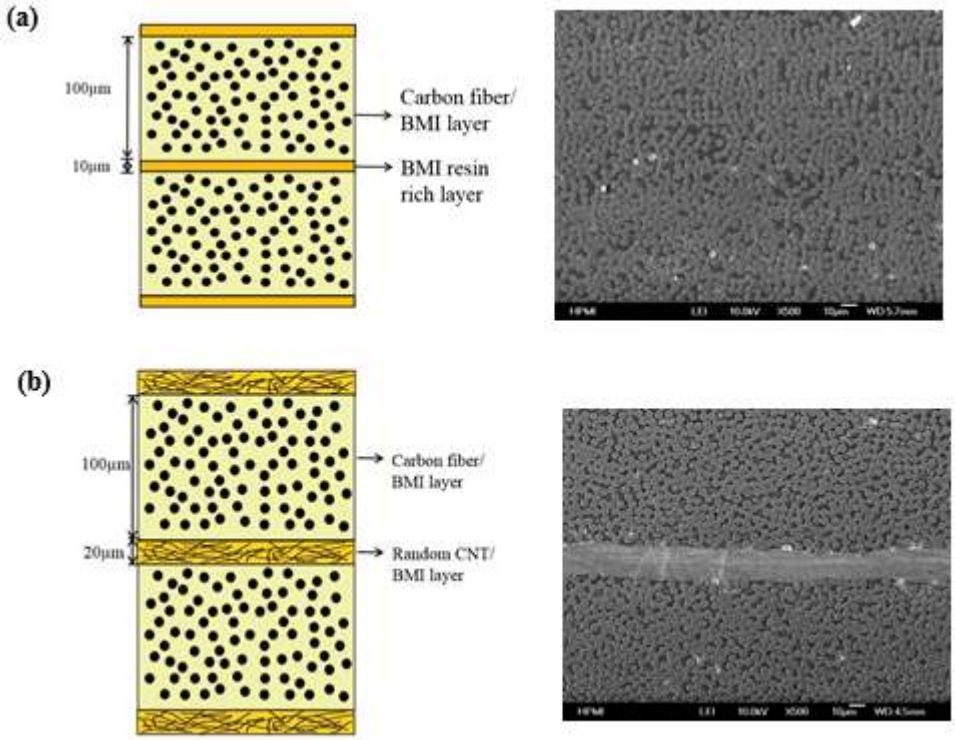

Figure 3. Cross-section morphologies and corresponding cartoon illustrations of the (a) CF- control and (b) BP/CF hybrid composites

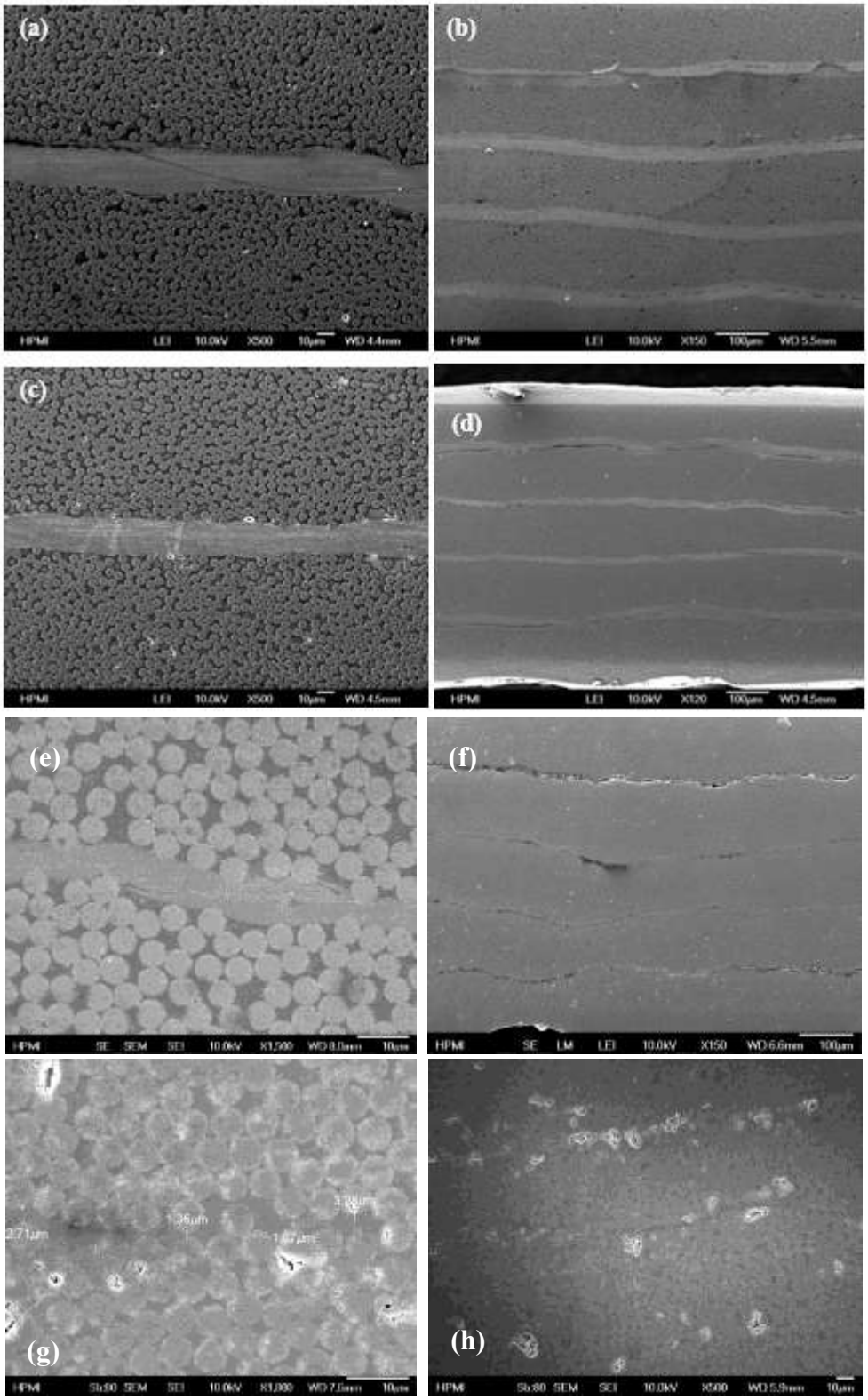

Figure 4. Cross-section morphologies of (a,b) NC-BP/CF, (c,d) functionalized NC-BP/CF, (e,f) FSU-BP/CF and (g,h) CVD-BP/CF hybrid composites, showing composite quality and interply structure

2.2. MECHANICAL PROPERTIES OF HYBRID COMPOSITES

Figure 5 shows the typical three-point bending stress-strain curves of the hybrid and corresponding control CF composite panels. The control unidirectional CF samples showed a linear elastic behavior

until the stress reached the maximum or peak load. Before the peak load, an audible cracking sound was heard due to the crack growth. Once the peak load was reached, the sample reached a maximum of 3 flexural cycles before the CF failed via brittle fracture and "V" shaped permanent deformation was imposed. BP/CF hybrid composites reinforced by both carbon fiber and carbon nanotubes exhibited a different stress- strain profile, as shown in Figure 5. As the strain increased, the stress-strain curve deviated from the linear proportionality, and the material reacted plastically. This is likely caused by CNT re-orientation under flexural loading and slippage at the CNT/resin interface and the BP/CF interface. The interface between the functionalized BP and CF remained strong enough to retain the macro-structure integrity under a non-stressed state. Table 2 summarizes both tensile and flexural properties of hybrid composites. Among three different BP cases, CVD-BP/CF hybrid composite exhibited the best mechanical properties.

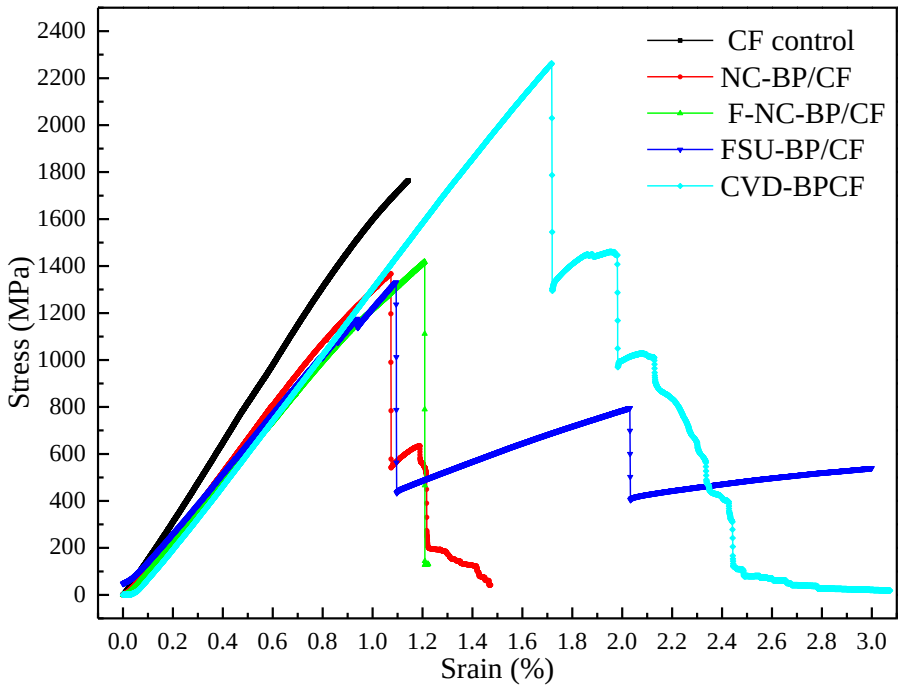

Figure 5. Typical three-point bend stress-strain curves the BP/CF hybrid composites and corresponding control samples

Table 2. Mechanical performances of BP/CF hybrid composites and corresponding control samples

Panel #	Name	Density (g/cm^3)	Tensile Strength (MPa)	Tensile Modulus (GPa)*	Flexural Strength (MPa)	Flexural Modulus (GPa)
1	CF control	1.61	2626±187	159±24	1763±32	157±3
2	BP control	1.49	331±25	18±2	-	-
3	NC-BP/CF	1.58	2519±101	150±8	1368±39	121±6
4	F-NC-BP/CF	1.58	2732±51	181±20	1401±40	131±8
5	FSU-BP/CF	1.55	2755±103	144±2	1316±36	127±14
6	CVD-BP/CF	1.59	2978±101	139±2	2183±264	144±12

2.3. ANALYSIS ON FAILURE MODES

The failure modes of the hybrid composites and corresponding CF control under three- point bending loads was studied via SEM analysis. The CF control sample resulted in a brittle failure as shown in Figure 6. The cross- sectional morphology of the failure clearly shows the CF strands broken cleanly at varied lengths which is the typical failure mode of carbon fiber composites under flexural load.

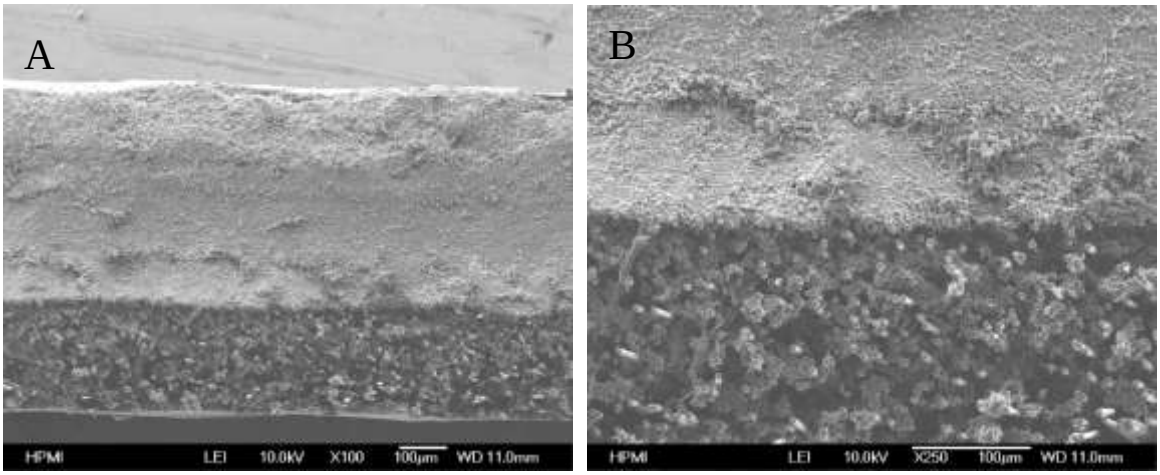

Figure 6. Three-point bending failure cross section of CF control. (a) The full sample cross sectional failure and (b) the CF failure plane at increased magnification

To compare, the addition of the BP layer that exhibits a delamination failure in Figure 7 where the CF layers are broken in a brittle fashion as seen before but mixed with the pull-out failure of the BP layer. The BP layer does not demonstrate typical CNT fracture. CNT composite failure is due to slippage of the CNT/resin interface and is visibly seen through nanotubes sliding out and are left freely suspended at the fracture edge.

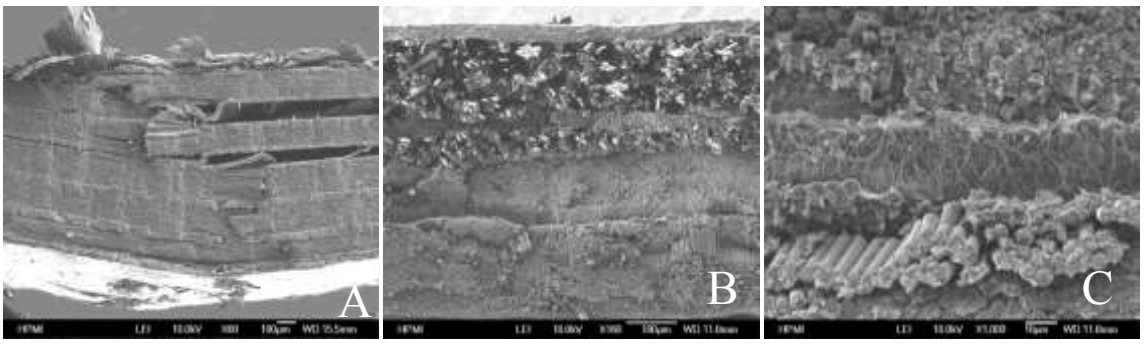

Figure 7. Three-point bending failure of random BP/CF hybrid exhibiting (a) delamination macro-scale failure, (b) visible layer differentiation of BP and CF, and brittle and (c) pullout failures of the CF and CNT

When the BP was also functionalized, a more complex fracture morphology is revealed in Figure 8. Not only is an interlaminar delamination failure seen as before in Figure 7, but the addition of the epoxidation treatment on the BP demonstrates increased interfacial adhesion between the BP and CF layers. Even more, cracks that propagate along the CF/resin layers are halted by the BP layer because of the pore and fiber size differences between the CF and BP that do not allow the cracking to transmit through layers.

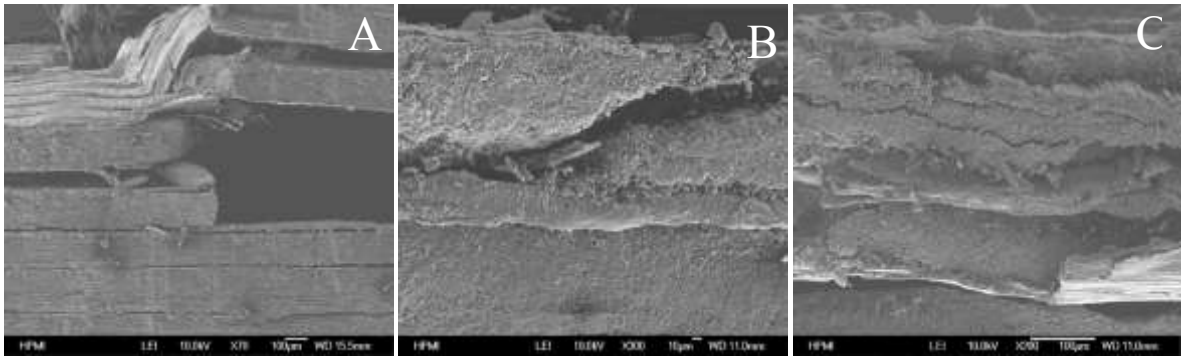

Figure 8. Three-point bending failure of functionalized BP/CF hybrid showing (a) delamination failure, (b) interply separation of BP/CF layers and (c) crack propagation behavior

2.4. ELECTRICAL CONDUCTIVITY OF BP/CF HYBRID COMPOSITES

One of the major advantages that CNTs have is the high electrical conductivity of individual nanotubes that can be translated into high CNT content composites. Table 3 shows the electrical conductivities of BP/CF hybrid and control composite samples. The in-plane electrical conductivity of the UD-CF in the axial direction of control sample was 94.5 S/cm. After applying NC-BP, the electrical conductivity of the NC-BP/CF hybrid composite increased to 459 S/cm. The functionalized NC-BP/CF with the same vol% of CNTs showed a slight decrease in electrical conductivity of 378 S/cm. Fiber transverse direction and out-of-plane electrical conductivities of the hybrid composites showed even better improvements, which benefitted from both high electrical conductivity of buckypaper and its bridging effect to the adjacent carbon fibers. In the transverse direction, the electrical conductivity of NC-BP/CF improved the most dramatically by almost 700 times. The out of plane electrical conductivity is an attractive addition to the multifunctional properties that the addition of the BP layer adds, where the electrical conductivity shows an increase of almost double in the case of the BP/CF hybrid. Table3 ultimately shows that orientation, functionalization and BP vol% can be tailored to a desired conductivity in three planes.

Table 3. Electrical conductivity of the BP/CF hybrid composites and corresponding control samples

Panel #	**Name**	**In-plane electrical conductivity [S/cm]**		**Out-of-plane electrical conductivity [S/cm]**
		Axial	Transverse	
1	CF control	94	0.13	0.040
2	BP control	620	620	-
3	NC-BP/CF	459	90	0.072
4	F-NC-BP/CF	378	56	0.057

3. CONCLUSIONS

It has been shown how BP layers can be integrated into CF traditional composites to create a new class of hybrid composites. It is the goal of these hybrid composites to increase the electrical, tensile and flexural properties compared to CF composites (the control samples) that can be manufactured on a large scale that can be realized in industrial applications. These nano/micro hybrid composites

demonstrated how there is a new dual-scale resin flow characteristic due to the surprisingly high BP swelling effect in comparison to the CF in a pressurized resin environment. By incorporating three linds of CNT materials, hybrid composites exhibited excellent mechanical properties, meanwhile harvested markedly enhanced electrical properties along the 3 planes due to BP content and orientation effects. The vast improvements in both in-plane and through-thickness electrical conductivities when BP layers introduced validate that the addition of the BP layer has a future for multifunctional composite applications. The strong CNT capillary effect in the hybrid composites absorbed a large amount of resin that voids were found inside the CF layers. This new discovery has proven that to be able to overcome the strong capillary absorbtion at the nanoscale level, an innovative approach must be taken to the manufacturing process of the hybrid composites. The resin, CNT and CF contents and multiscale resin flow during manufacturing must be considered in order to achieve high-quality and high-performance of the parts.

ACKNOWLEDGEMENTS

This work was also partially supported by NSF Scalable Nanomanufacturing Program project (SNM 1344672) and AFOSR FA9550-17-1-0005 project. We thank Mr. Frank Allen for critical reviewing of the manuscript. C. Jolowsky and R. D. Sweat would like to thank the fellowship supported by Solvay-Cytec Engineering Materials.

REFERENCES

[1] J.N. Coleman, U. Khan, W.J. Blau, Y.K. Gun'ko, Small but strong: A review of the mechanical properties of carbon nanotube–polymer composites, Carbon. 44 (2006) 1624–1652. doi:10.1016/j.carbon.2006.02.038.

[2] Z.-G. Zhao, L.-J. Ci, H.-M. Cheng, J.-B. Bai, The growth of multi-walled carbon nanotubes with different morphologies on carbon fibers, Carbon. 43 (2005) 663–665.

[3] E.T. Thostenson, C. Li, T.-W. Chou, Nanocomposites in context, Compos. Sci. Technol. 65 (2005) 491–516. doi:10.1016/j.compscitech.2004.11.003.

[4] M. Endo, H. Muramatsu, T. Hayashi, Y.A. Kim, M. Terrones, M.S. Dresselhaus, Nanotechnology: "Buckypaper" from coaxial nanotubes, Nature. 433 (2005) 476–476. doi:10.1038/433476a.

[5] Q. Cheng, B. Wang, C. Zhang, Z. Liang, Functionalized Carbon-Nanotube Sheet/Bismaleimide Nanocomposites: Mechanical and Electrical Performance Beyond Carbon-Fiber Composites, Small. 6 (2010) 763–767. doi:10.1002/smll.200901957.

[6] I.-W.P. Chen, Z. Liang, B. Wang, C. Zhang, Charge-induced asymmetrical displacement of an aligned carbon nanotube buckypaper actuator, Carbon. 48 (2010) 1064–1069. doi:10.1016/j.carbon.2009.11.026.

[7] Q. Wu, J. Bao, C. Zhang, R. Liang, B. Wang, The effect of thermal stability of carbon nanotubes on the flame retardancy of epoxy and bismaleimide/carbon fiber/buckypaper composites, J. Therm. Anal. Calorim. 103 (2010) 237–242. doi:10.1007/s10973-010-0960-0.

[8] J.W. Bao, Q.F. Cheng, X.P. Wang, Z.Y. Liang, B. Wang, C. Zhang, L. Kramer, P. Funchess, D. Dorough, Mechanical properties of functionalized nanotube buckypaper composites, in: 17th Int. Conf. Compos. Mater., 2009. http://www.iccm-central.org/Proceedings/ICCM17proceedings/Themes/Nanocomposites/CARBON%20NANOTUBE%20COMPOSITES/E1.31%20Liang.pdf (accessed September 23, 2015).

[9] Q. Cheng, J. Bao, J. Park, Z. Liang, C. Zhang, B. Wang, High Mechanical Performance Composite Conductor: Multi-Walled Carbon Nanotube Sheet/Bismaleimide Nanocomposites, Adv. Funct. Mater. 19 (2009) 3219–3225. doi:10.1002/adfm.200900663.

[10] S. Wang, R. Downes, C. Young, D. Haldane, A. Hao, R. Liang, B. Wang, C. Zhang, R. Maskell, Carbon Fiber/Carbon Nanotube Buckypaper Interply Hybrid Composites: Manufacturing Process and Tensile Properties, Adv. Eng. Mater. 17 (2015) 1442–1453. doi:10.1002/adem.201500034.

[11] H. Xu, X. Tong, Y. Zhang, Q. Li, W. Lu, Mechanical and electrical properties of laminated composites containing continuous carbon nanotube film interleaves, Compos. Sci. Technol. 127 (2016) 113–118. doi:10.1016/j.compscitech.2016.02.032.
[12] X. Fu, C. Zhang, T. Liu, R. Liang, B. Wang, Carbon nanotube buckypaper to improve fire retardancy of high-temperature/high-performance polymer composites, Nanotechnology. 21 (2010) 235701. doi:10.1088/0957-4484/21/23/235701.
[13] J.G. Park, J. Louis, Q. Cheng, J. Bao, J. Smithyman, R. Liang, B. Wang, C. Zhang, J.S. Brooks, L. Kramer, P. Fanchasis, D. Dorough, Electromagnetic interference shielding properties of carbon nanotube buckypaper composites, Nanotechnology. 20 (2009) 415702. doi:10.1088/0957-4484/20/41/415702.
[14] R. Downes, S. Wang, D. Haldane, A. Moench, R. Liang, Strain-Induced Alignment Mechanisms of Carbon Nanotube Networks, Adv. Eng. Mater. 17 (2015) 349–358. doi:10.1002/adem.201400045.
[15] S. Wang, D. Haldane, R. Liang, J. Smithyman, C. Zhang, B. Wang, Nanoscale infiltration behaviour and through-thickness permeability of carbon nanotube buckypapers, Nanotechnology. 24 (2013) 015704.